Acoustic Timing Simulation of Active Beacons for Measuring the Tow-Path of a Synthetic Aperture Sonar

Edward N. Pilbrow and Michael P. Hayes
Acoustics Research Group:
Dept. Electrical and Computer Engineering,
University of Canterbury,
Te Whare Wananga o Waitaha,
Private Bag 4800, Christchurch, NEW ZEALAND.
{e.pilbrow,m.hayes}@elec.canterbury.ac.nz

Abstract

A simulation of freely-deployed active underwater beacons to estimate the tow path of a Synthetic Aperture Sonar (SAS) towfish is presented. Knowledge of the tow path allows the removal of motion induced blurring in the SAS images. The beacons sit on the seabed listening for acoustic chirps from the sonar and retransmit back in a different frequency band after a fixed time delay. After reconstruction the beacons appear in the SAS image as point-source targets, blurred by towfish motion, from which the tow-path can be determined by triangulation. The effect of reconstructing the continuous towfish motion as discrete along-track 'hops' is also investigated. Simulations of a towfish path with 20 cm sway amplitude and typical measurement timing errors show a significant improvement in image quality using two active beacons.

Keywords: SAS, simulation, timing, flight time, path, reconstruction

1 Introduction

Synthetic Aperture Sonar (SAS) is a technique for high-resolution, range-independent sea floor imaging. However, image quality is severely degraded by unknown motions of the sonar [1] with magnitudes greater than 1/10 th of the imaging wavelength [2]. If the path of the sonar through the water could be measured, the motion-blur could be removed by post-processing the image. Current approaches to estimating the sonar motion include the use of inertial navigation systems [3] and data-driven autofocus techniques [4], but verifying the results is difficult in an underwater environment. We propose to deploy acoustic 'active beacons' on the sea floor [5] that listen for the sonar signal and retransmit in a different frequency band. This will provide an independent set of data [6] that can be used to verify the sonar path. The beacons are currently under construction and will operate with the KiwiSAS-IV towfish, designed and built at the University of Canterbury, New Zealand. Figure 1 shows the previous sonar, KiwiSAS-III, which is similar in basic operation to the KiwiSAS-IV but without an additional hydrophone array.

We start by explaining how the sonar/beacon system works in Section 2 and then derive the time of flight equations for a moving sonar in Section 3. The result is compared to the traditional 'stop and hop' model and simplified versions of the equations are shown that closely model the error between the two methods. Section 4 shows the reconstructed data from SAS simulations of a dual beacon system using time of flight data to remove the towfish wobble. Finally, a discussion of the limitations of the model used is given in Section 5.

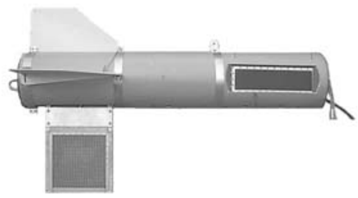

Figure 1: The KiwiSAS-III towfish. The rectangular transmitter is mounted within the body at the front while the square receiver keel hangs down below the fins at the rear.

2 Active beacon operation

Figure 2 shows a photo of an active beacon as it would be deployed on the seabed and Figure 3 shows a plan view of the deployment in relation to the sonar tow path. Using a number of these beacons enables the towfish path through the water to be measured, allowing the motion blur to be removed from the SAS images.

The beacon system is capable of measuring both one-way and two-way flight times [7]. This is illustrated in

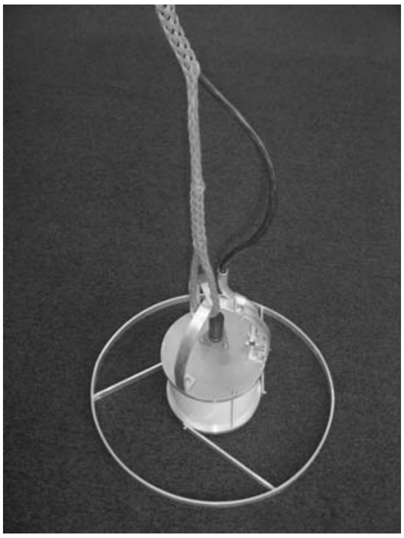

Figure 2: The beacon is freely deployed to sit on the seabed in the area of interest, connected by a cable to a control unit floating on the surface. A cylindrical hydrophone on the top alternately acts as a receiver and transmitter, listening for each sonar chirp, and replying back at a different frequency after a fixed delay. GPS timing receivers in the beacons and the towfish ensure all points of measurement are synchronized. The beacons transmit between each other (when the sonar is not doing an imaging run) to determine their separation.

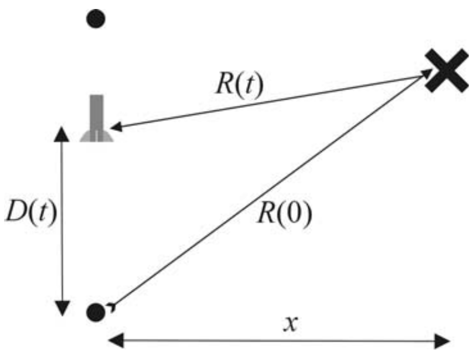

Figure 3: Plan view of the towfish traveling up the page with the start of transmission of each chirp represented by a black dot. The across-track separation, x, between the sonar and the beacon is assumed constant. The black cross is a beacon at (x_b, y_b) that listens for sonar chirps and retransmits them in a different frequency band after a constant time delay due to the internal electronic processing involved. Each beacon will use a different chirp signature to allow individual identification by matched-filtering.

Figure 3 where the one-way flight path is $R(0)$ and the two-way path is $R(0)+R(t)$. Each beacon continuously samples the signal received by its transducer. When a sonar chirp is detected, a matched filtering technique is used to determine its time of arrival. The beacon sends this time information up the cable to a floating surface unit where it is transmitted to the towboat via an RF modem for storage.

After the matched filtering has been performed, the beacon transmits a chirp back to the sonar, using the transducer as a transmitter. A different frequency band is used to enable the sonar to distinguish the beacon chirps from the reflected signals from other passive targets on the seabed. The time between reception of a chirp and transmission back to the sonar is a known constant delay. The beacon chirps are received by the sonar and reconstructed to form a separate SAS image of high intensity point-like targets. With knowledge of the beacon separation and the time delay inherent in each beacon, the towfish position at every chirp can be calculated by triangulation. The simulation in Section 4 models this two-way flight path.

To remove the motion blur, an arbitrary straight tow path is chosen and the necessary time-shifts to align each beacon chirp onto the straight path are calculated. The same shifts are then applied to each received echo from the passive targets thus removing the motion blur from the passive SAS images.

The correction achieved by simply time shifting each chirp is not perfect because the shifts are all in a particular direction whereas the chirps are radial measurements, i.e., for a particular received echo, a target at broadside will be shifted by the correct amount but those to each side will be shifted by less than the correct amount. However, the comparatively narrow beam pattern of the sonar means the echo amplitude from targets at angles not close to broadside is low so the distortion is minimal. The effect can be seen in Figure 4 where the target is located at (20,-5) and the corrected range curve is a smooth hyperbola at broadside to this point but distorts as the sonar travels further along-track. Further improvement in image quality can be achieved by using autofocus techniques [4] that would otherwise be unable to operate successfully on images with motion blur present.

2.1 Reconstruction of two-way timing data

One way timing data theoretically provides the most accurate measurement of the towfish position at each point because it is a single measurement initiated at one instant[1]. However, this is not the way the SAS images

[1]Although the sonar moves during the 12.5 ms transmission, this effect is not significant.

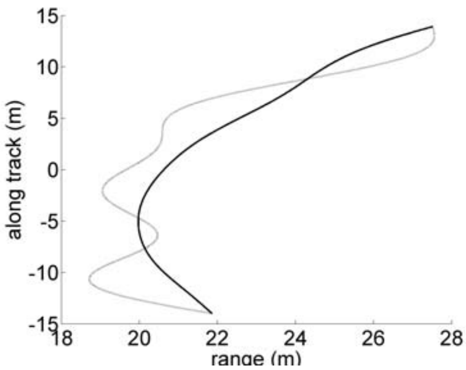

Figure 4: Range from the sonar to a target located at (20,-5) before (faint line) and after (solid line) correction of the wobbled towpath to a straight line by time shifting each chirp. A perfect straight towpath produces a hyperbola in range. The solid line here is not a perfect hyperbola because the time shift for each ping is performed in the across-track direction whereas the range is measured in a radial direction.

are formed. SAS measures a two-way reflection from the sonar to a target and back to the sonar, corrupted by towfish motion and medium fluctuations occurring during this time. Measuring the path of the sonar using two way timing data includes the effects of towfish interping motion and medium fluctuations so may prove to produce better deblurring of the SAS images.

At sea, the sonar is moving so a two way measurement is made but, for simplicity, the data is reconstructed assuming the sonar is stationary between transmitting and receiving each ping, i.e., assuming a one-way path. The next section derives an expression for the error in this approach and includes the effect of a time delay associated with the active beacons.

3 Propagation time equations

The following equations are derived from Figure 3 showing the sonar motion approximated by a straight path of constant speed, v, between two points where chirp transmission occurs. Although the equations are derived for a constant across-track separation between the sonar and the beacon, i.e., constant x, the coordinate system can be rotated for each ping to approximate an arbitrary path as a series of straight paths between transmissions.

3.1 Transmit receive hop model

In the Transmit Receive Hop model (TRH), also known as ‘stop and hop’, the continuously moving sonar is modelled as remaining at a fixed position while transmitting a chirp and receiving the response back from the beacon. It then hops instantaneously to the next ping position along the towpath and the cycle repeats. This is the model used in the Fourier transform based reconstruction algorithms. If transmission of a chirp commences at $t = 0$ then the total propagation time from the sonar to the beacon plus an electronic processing delay, τ_{beacon}, and transmission back to the sonar is

$$\tau_{\text{TRH}}(t) = \frac{1}{c}\left[2R(0)\right] + \tau_{\text{beacon}}, \tag{1}$$

where c is the speed of sound in seawater and $R(0)$ is the range from the beacon to the sonar.

3.2 Transmit hop receive hop model

Under the Transmit Hop Receive Hop (THRH) model, movement between transmission and reception is modelled but the movement during transmission and reception of each ping is ignored. The sonar is modelled as remaining in a fixed position while transmitting a chirp then hops instantaneously to the point along the path where it will receive the first part of the response from the beacon. It then hops instantaneously to the next ping position along the towpath and the cycle repeats. The total propagation time is

$$\tau_{\text{THRH}}(t) = \frac{1}{c}\left[R(t) + R(0)\right] + \tau_{\text{beacon}}, \tag{2}$$

where $R(t)$ is the range from the beacon to the sonar when the sonar is receiving. By similar triangles we see that

$$R^2(t) = R^2(0) + D^2(t) + 2D(t)\left[y_b - (y(0) + D(t))\right], \tag{3}$$

where $D(t)$ is the along-track hop of the sonar from $y(0)$ during $\tau_{THRH}(t)$ and y_b is the along-track position of the beacon. Substituting

$$D(t) = v\tau_{\text{THRH}}(t) = a\left[R(t) + R(0)\right] + v\tau_{\text{beacon}}, \tag{4}$$

where $a = v/c$ into Equation 3 and solving gives

$$R(t) = \alpha + \sqrt{\alpha^2 + \beta}, \tag{5}$$

where

$$\alpha = \frac{a\left[y(0) - y_b + \Delta + aR(0)\right]}{1 - a^2}, \tag{6}$$

$$\beta = \frac{R(0)^2\left(1 + a^2\right) + \Delta^2 + 2aR(0)\Delta}{1 - a^2} + \frac{\left(2aR(0) + 2\Delta\right)\left(y(0) - y_b\right)}{1 - a^2}. \tag{7}$$

where $\Delta = v\tau_{\text{beacon}}$.

3.3 Total propagation time error

The difference in propagation time between the TRH and THRH models is

$$\begin{aligned} \tau_{\text{error}}(t) &= \tau_{\text{THRH}}(t) - \tau_{\text{TRH}}, \\ &= \frac{R(t) - R(0)}{c}. \end{aligned} \tag{8}$$

Substituting (5) into (8) gives

$$\tau_{\text{error}}(t) = \frac{1}{c}\left(\psi + \sqrt{\psi^2 + \gamma}\right), \tag{9}$$

where

$$\psi = \frac{-R(0) + 2a^2R(0) + a\Delta + a\,(y(0) - y_b)}{1 - a^2}, \tag{10}$$

$$\begin{aligned} \gamma = {} & \frac{4a^2R(0)^2 + 4aR(0)\Delta + \Delta^2}{1 - a^2} \\ & + \frac{(4aR(0) + 2\Delta)\,(y(0) - y_b)}{1 - a^2}. \end{aligned} \tag{11}$$

It can be shown that for any value of τ_{beacon}, this formula is identical to that of a towfish with a receiver and transmitter separated in the along-track direction by Δ if the sonar is imaging a passive target, i.e, a target with no inherent delay.

If the coordinate system is adjusted so that $y_b = 0$ and a typical SAS geometry like that shown in Table 1 is used, $\tau_{\text{error}}(t)$ can be approximated by an equation of the form

$$\tau_{\text{error}}(t) = my(0) + C, \tag{12}$$

where

$$m = -\frac{2a}{c} - \frac{\Delta}{cR(0)}, \tag{13}$$

$$C = \frac{a\Delta}{c}, \tag{14}$$

giving an approximation error of less than 600 ns over the tow path shown in Figure 6.

The effect of $\tau_{\text{error}}(t)$ is to skew the image in the along-track direction when reconstruction is done using the TRH model. This can be approximately corrected by steering the synthetic beam forward by an angle of $2a$.

4 Simulation method

A Fourier transform based simulation using the two way time of flight data from Equation 9 has been written in Matlab to simulate a sea floor image containing two beacons, blurred by a wobbled towfish tow path[2].

[2]In a typical seabed image there would be background noise, multipath, and other passive targets present but for simplicity here we use just the two beacons as both active and passive targets.

Table 1: Simulated operating parameters of the KiwiSAS towfish and proposed active beacons.

Chirp length	12.5 ms
Chirp repeat period	68 ms (approx)
Chirp bandwidth	20 kHz
Chirp center frequency	30 kHz
Sampling frequency	30 kHz
Samples per chirp	2048
Number of chirps	512
Sonar along-track velocity	0.8 m/s
Sonar transmitter length	0.3 m
Sonar receiver length	0.3 m
Speed of sound	1500 m/s
Number of beacons	2
Beacon locations	(20,-5,0), (25,4,0)
Absolute timing errors	10 μs
Relative timing errors	1 μs RMS
Beacon separation error	1 cm
Beacon processing delay	50 ms

For every chirp transmitted by the sonar a signal is received back and, after matched-filtering, a number of peaks are identifiable as shown in Figure 5. The highest corresponds to the chirp transmitted by the particular beacon identified by the matched-filter signature. Lower peaks are from reflections off other passive objects and transmissions from other beacons with different chirp signatures. The amount to shift each image slice to straighten up the towpath can be accurately determined by interpolating to find the true peak. The shift is then applied to the passive image of the seabed. In this example the passive image contains only the two beacons.

The simulation parameters for the KiwiSAS sonar are listed in Table 1. Although the simulation is two dimensional and does not simulate the changing towfish depth, pressure sensors in the towfish and beacons allow this to be corrected with real data.

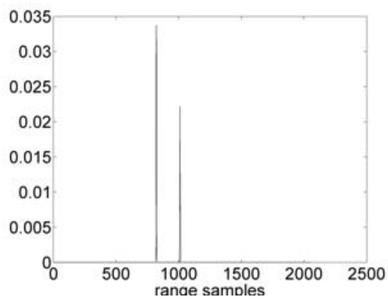

Figure 5: Typical slice through the unreconstructed image of the scene of Figure 6 showing the received signal for a single chirp. The high peak in the correlation envelope belongs to the beacon identified after matched-filtering with its signature chirp. The peak position allows the time of arrival to be calculated after sub-sample interpolation.

4.1 Results

The simulated tow path with wobble is shown in Figure 6. This is a typical path for the KiwiSAS towfish on a calm day. The motion is a combination of the undersea currents acting on the towfish and the surface waves acting on the tow boat and has a maximum peak to peak sway of 40 cm.

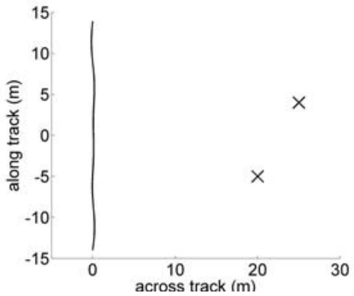

Figure 6: Tow path with wobble and the location of two active beacons used in the simulation.

4.1.1 Results - no timing errors

Figure 7 shows the reconstruction of the data from Figure 6 when there are no errors in any of the timing measurements. If no correction is performed, as in Figure 7(a), the sonar wobble smears the peaks in the along-track direction and shifts the highest point well away from its correct location. Using the one-way time of flight data to correct for the sonar wobble produces the image in Figure 7(b). Although there is still some along-track smearing, the peak is easy to see (28.4 dB above the side-lobes) and located in the correct position. The perfect result, i.e., if the sonar had taken a straight path through the water, is shown in Figure 7(c).

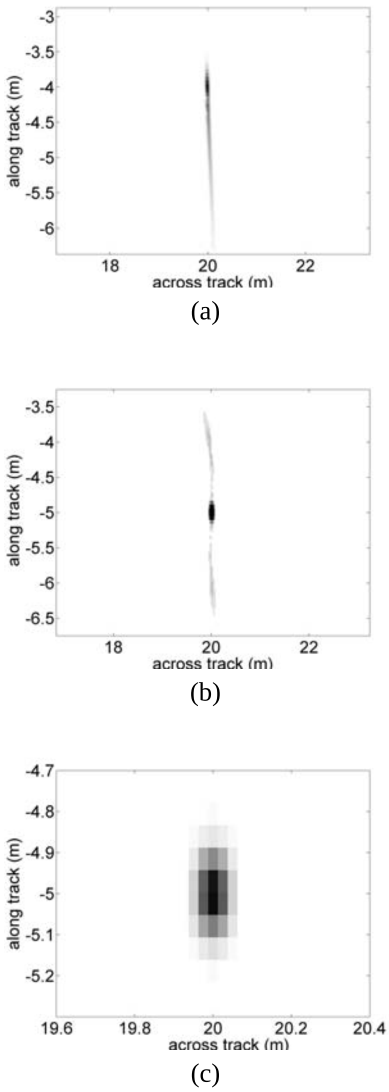

Figure 7: Reconstructed image with (a), no correction and (b), correction by triangulation with the two beacons. Image (c) shows the perfect result, i.e., if no wobble had been present.

4.1.2 Results - timing errors

In practice, any real timing measurements made will have some associated uncertainty due to the background sea noise, accuracy of the GPS timing reference, component tolerances, and calibration errors. To simulate this, three types of timing errors were added to the time of flight measurements before reconstruction. Table 1 shows the values expected [8] with the KiwiSAS active beacons. 'Absolute timing errors' affect both beacons equally, e.g., an estimate of the speed of sound. 'Relative timing errors' are different in both beacons, e.g., GPS timing errors. 'Beacon separation error' refers to the error in acoustically measuring the distance between the beacons. When all of these errors are simulated, the image of Figure 7(b) degrades to that in Figure 8. The side lobes have increased in amplitude but are still 21.8 dB below the peak and the peak is close to the correct location.

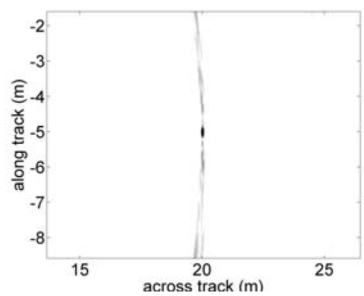

Figure 8: Reconstructed image after correction when measurement timing errors are included as discussed in Section 4.1.2

4.1.3 Results - beacon delay

Including the effects of a beacon internal processing delay requires a two-way time of flight simulation to determine the exact point at which the towfish receives the chirp from each beacon. A shear to the image occurs when a TRH reconstruction is used as explained in Section 3.3. This can be seen in Figure 9 where the peak has shifted in the negative along-track direction.

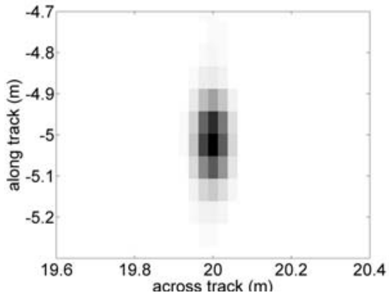

Figure 9: Reconstructed image after correction when a beacon delay is included. The image has been sheared in the along-track direction.

5 Discussion

Although the THRH simulator models the SAS process significantly better than a TRH simulator, there are still a number of minor phenomena that are ignored. This is done for simplicity and speed of simulation, particularly when it comes to calculating the beam pattern which varies with target position and look-angle. The sonar moves during transmission and reception but the beam pattern for each target is simulated at a fixed towfish position for every chirp causing a slight decorrelation of the received echo.

A Doppler shift occurs with the received and transmitted chirps due to the fact that the sonar is moving while transmitting and receiving. This is due to the very small velocity component of the sonar directly toward (when approaching a target) and away (after going past a target) from each target as it travels in a straight along-track direction. The simulator ignores this change in frequency. Finally, the simulator does not take into account the effects of multipath reflections from the seabed and sea surface. This produces additional peaks close to the first beacon peak but is not expected to be a significant problem because the direct path is always the shortest path, i.e., the first peak is chosen.

6 Conclusion

The use of active beacons with constant time delays between reception and retransmission of sonar chirps can be used to remove much of the blurring caused by a non straight towpath. Reconstructing the corrected images using a model that assumes the sonar hops discretely between transmissions causes a shearing of the image but still significantly improves the image quality.

References

[1] P. T. Gough and D. W. Hawkins. Imaging algorithms for a strip-map synthetic aperture sonar: minimising the effects of aperture errors and aperture undersampling. *IEEE Journal of Oceanic Engineering*, 22:27–39, 1997.

[2] D. W. Hawkins. *Synthetic Aperture Imaging Algorithms: with application to wide bandwidth sonar.* PhD thesis, Department of Electrical and Computer Engineering, University of Canterbury, October 1996.

[3] E. N. Pilbrow, P. T. Gough, and M. P. Hayes. Inertial navigation system for a synthetic aperture sonar towfish. In *Proceedings of Electronics New Zealand Conference*, Dunedin, New Zealand, 14-15 November 2002.

[4] P. T. Gough, M. P. Hayes, H. J. Callow, and S. A. Fortune. Autofocussing procedures for high-quality acoustic images generated by a synthetic aperture sonar. In *Proceedings of International Congress on Acoustics*, Rome, Italy, September 2001.

[5] E. N. Pilbrow, P. T. Gough, and M. P. Hayes. Dual transponder precision navigation system for synthetic aperture sonar. In *Proceedings of Electronics New Zealand Conference*, Dunedin, New Zealand, 14-15 November 2002.

[6] J. Pihl, P. Ulriksen, O. Kroling, B. Lovgren, and G. Shippey. MLO classification using an ROV-mounted wideband synthetic aperture sonar. In *Proceedings of The 5th European Conference on Underwater Acoustics*, Lyon, France, July 2000.

[7] E. N. Pilbrow and M. P. Hayes. Active sonar beacons to aid synthetic aperture sonar autofocussing: Beacon-controller design and performance. In *Proceedings of Electronics New Zealand Conference*, Hamilton, New Zealand, 1-2 September 2003.

[8] E. N. Pilbrow, P. T. Gough, and M. P. Hayes. Long baseline precision navigation system for synthetic aperture sonar. In *Proceedings of The 11th Australasian Remote Sensing and Photogrammetry Association Conference*, Brisbane, Australia, 3-5 November 2002.